Buddika 2020 Supplementary Figures

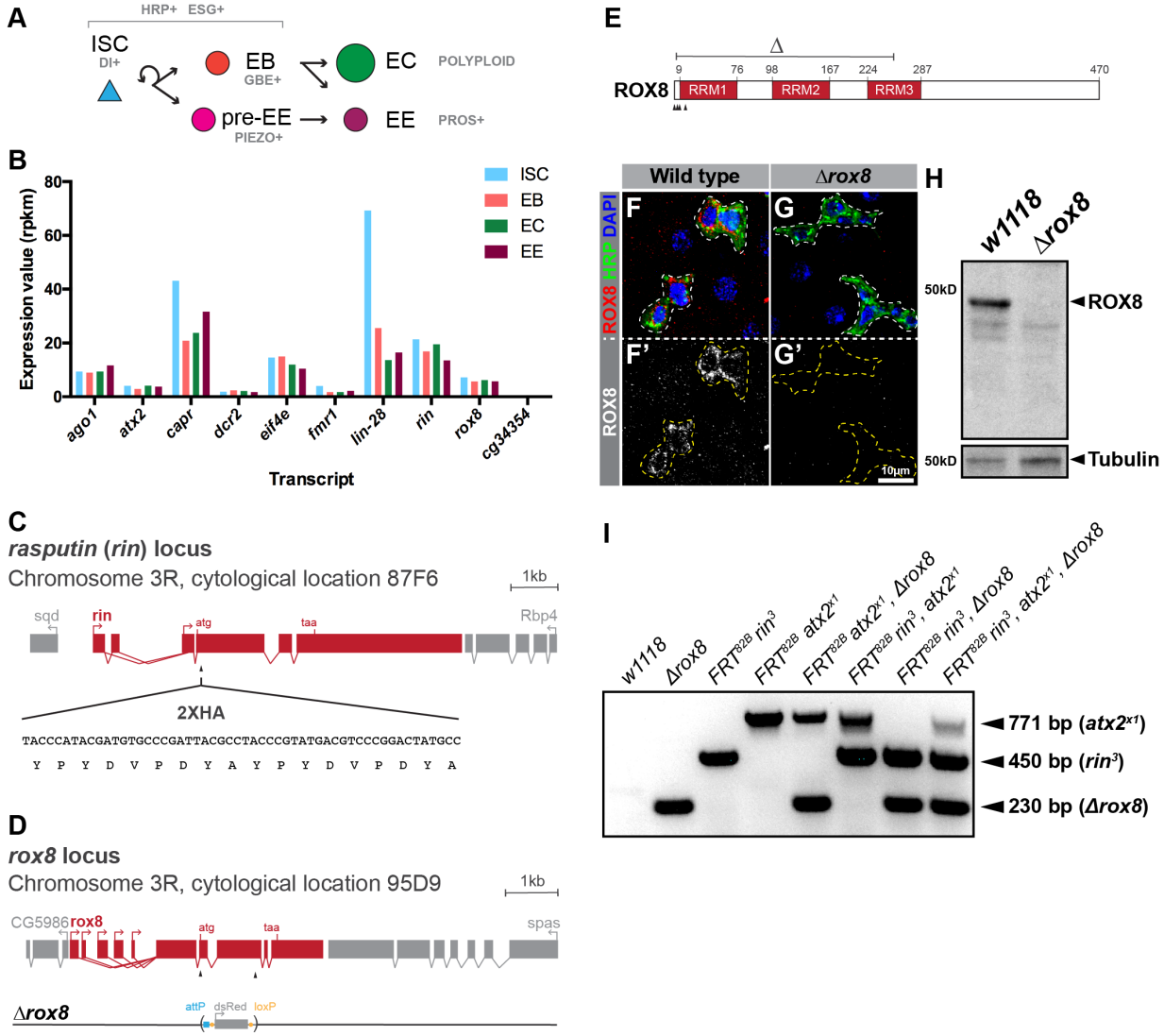

Figure S1: Background and reagent information relevant to this study. (A) Schematic showing the ISC lineage as well as markers used to label cell types in this lineage. (B) A histogram showing transcript expression levels of genes analyzed in this study based on data from Dutta et al., 2013. Note that *CG34354*, a likely paralog of *rox8*, is not expressed in intestinal cells. (C) Schematic of the *rin* locus, including the location of the gRNA (arrowhead) used to insert 2XHA sequence. (D) Schematic of the wildtype *rox8* locus (top) and the *Δrox8* mutant locus (bottom) generated via CRISPR/cas9 mutagenesis using two gRNAs and a repair plasmid. Arrowheads indicate the locations of the gRNAs. (E) Schematic of the ROX8 protein, which is 470 amino acids long and

encodes three RNA recognition motifs (RRMs) in its N-terminal half. The portion deleted by the *Δrox8* deletion is indicated (Δ). In addition to the Δ deletion, four additional alleles were generated that disrupt the predicted reading frame after the first, second, fourth, and nineteenth amino acids (indicated by arrowheads). However, none of these mutations affected ROX8 accumulation as detected by Western blot, suggesting that the currently annotated start methionine may not be used (although the next downstream methionine is located 20 amino acids into the 68 amino acid RRM1 domain. (F-G) Confocal micrographs of epithelial sections from (F) wild type or (G) *Δrox8* intestines stained for ROX8 (red in F-G, white in F'-G'), HRP (green) and DAPI (blue). Note that *Δrox8* intestinal progenitor cells have no visible ROX8 staining. (H) Western blot of w^{1118} (control) and *Δrox8* whole animal extracts probed with ROX8 (top panel) or Tubulin (bottom panel) antibodies. (I) An agarose gel showing the PCR-based verification of each single, double and triple mutants that were used in the current study. A 771bp, 450bp, and/or 230bp product confirms the presence of the $atx2^{X1}$, rin^{3}, and/or *Δrox8* mutation, respectively.

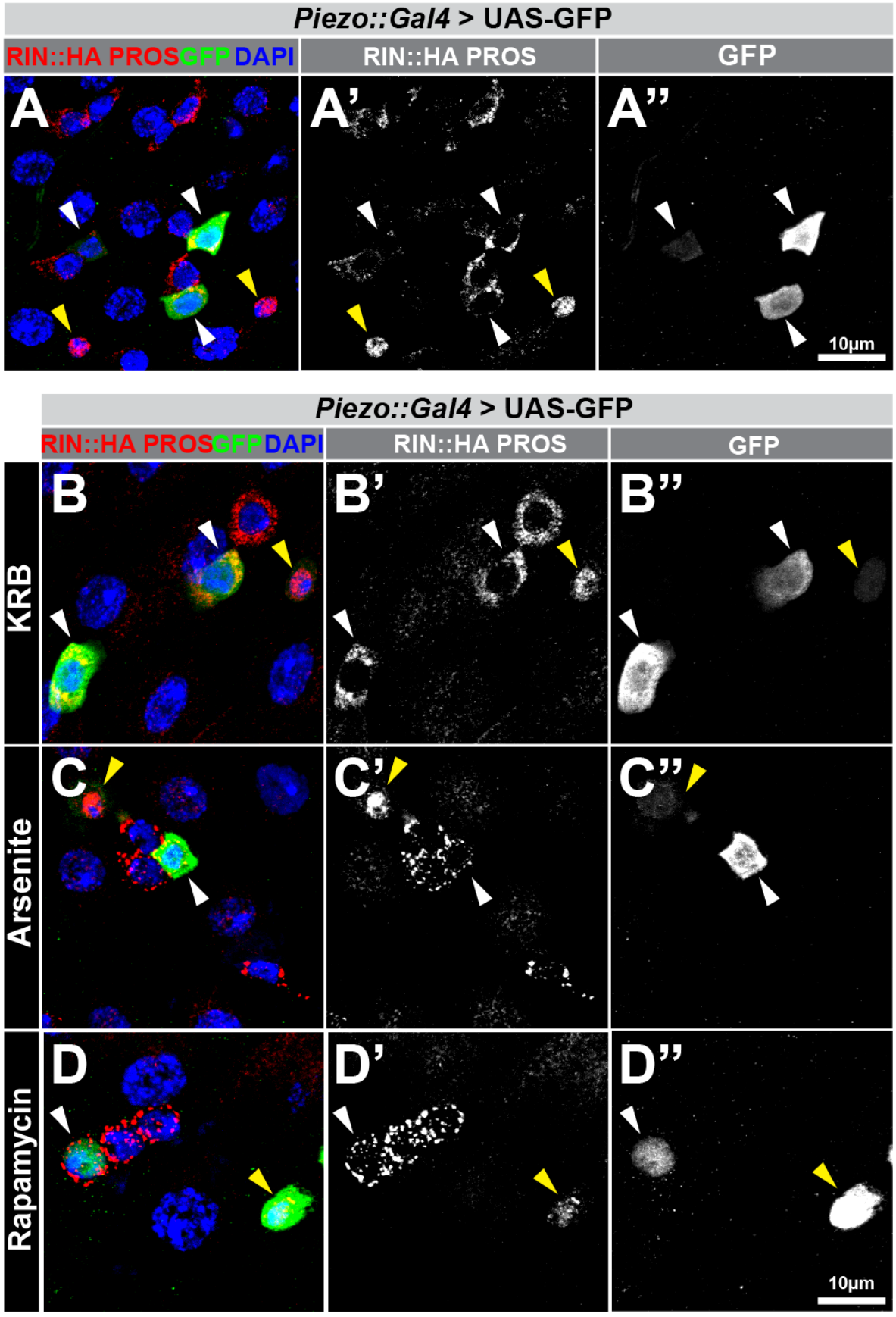

Figure S2: Stress granule proteins are expressed in EE precursors and are capable of assembling into mature stress granules following acute stress. (A) Confocal fluorescent micrographs of *piezo-Gal4>UAS-GFP* intestines stained for RIN-HA (red in A, white in A'), Prospero (red in A, white in A'), GFP (green in A, white in A"), and DAPI. While both RIN::HA and Pros were detected in the red channel, they could be distinguished based on distinct subcellular localization: RIN::HA was cytoplasmic while Pros was nuclear. Note that cytoplasmic RIN-HA staining was detected in Pros^{-}, *piezo*$^{+}$ EE precursors (white arrowheads in A') but not mature Pros+, *piezo*$^{-}$ EEs (yellow arrowheads in A'). (B-D) Confocal fluorescent micrographs of *piezo-Gal4>UAS-GFP* intestines treated with (B) KRB, (C) 1mM sodium arsenite, or (D) 1mM rapamycin and stained for RIN::HA (red in B-D, white in B'-D'), Pros (nuclear red in B-D, white in B'-D'), GFP (green in B-D, white in B''-D'') and DAPI (blue).

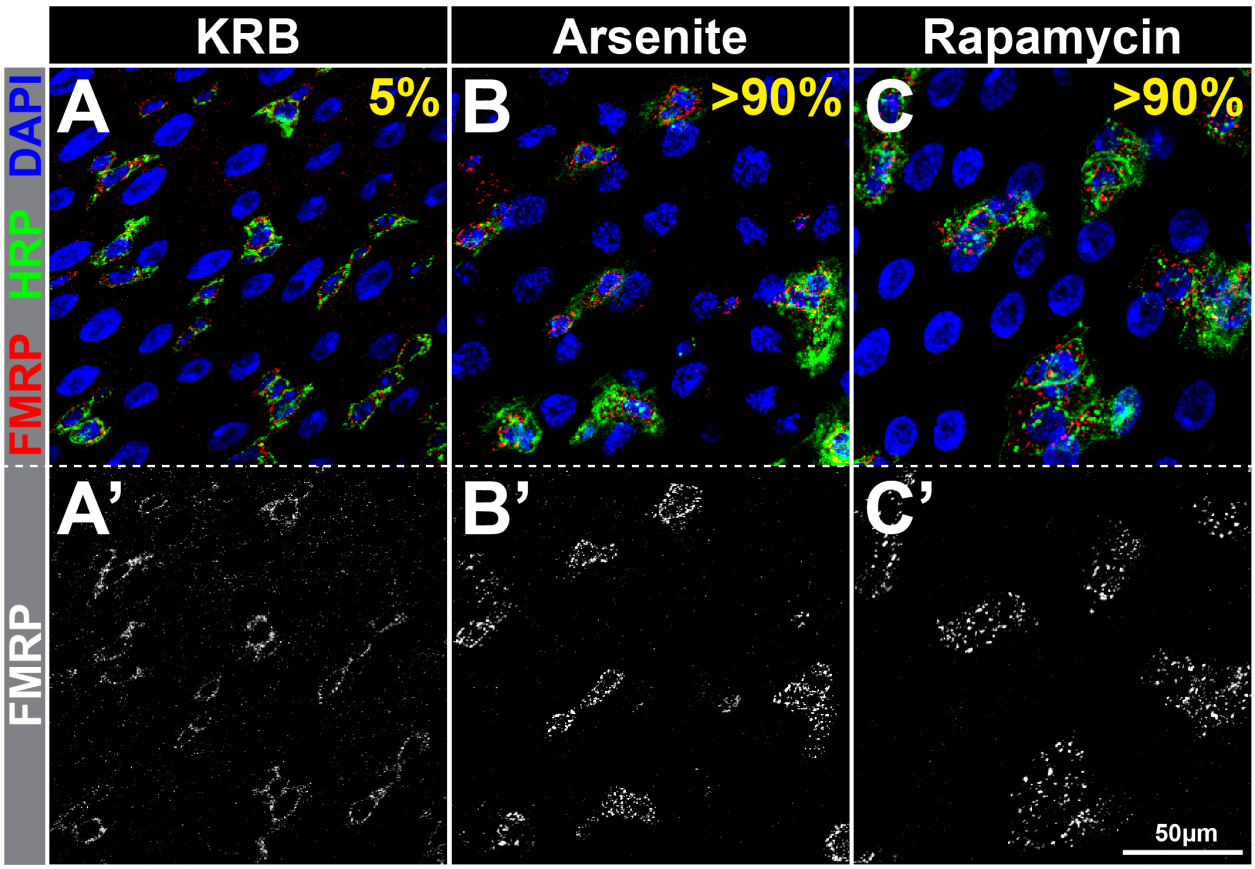

Figure S3: IPSGs are detected in >90% of intestinal progenitors after arsenite or rapamycin treatment. Fluorescent micrographs of a field of cells in the R5 region of wild type *Drosophila* intestines exposed to (A) KRB, (B) 1mM sodium arsenite or (C) 1mM rapamycin and stained for FMRP (red), HRP (green), and DAPI (blue). Single channel images of FMRP staining are shown in A'-C'. The numbers in yellow indicate quantification of the percentage of intestinal progenitors per field of view that display stress granules (n=5 intestines per condition).

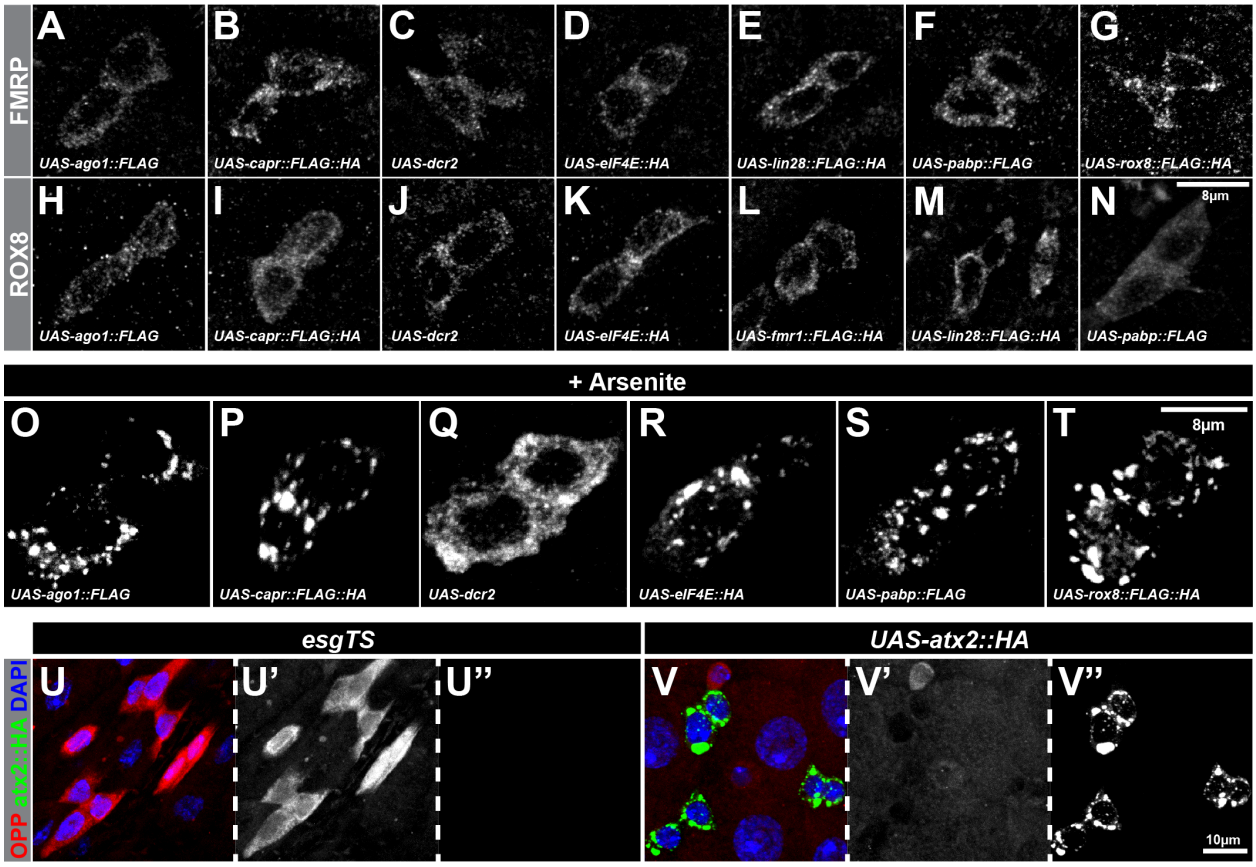

Figure S4: Forced expression of AGO1, CAPR, DCR2, eIF4E, FMRP, LIN-28 , pABP or ROX8 does not lead to IPSG formation. Gray scale images of pairs of progenitor cells from intestines harboring *esg-Gal4* and (A, H) *UAS-ago1::FLAG*, (B, I) *UAS-capr::FLAG::HA*, (C, J) *UAS-dcr2*, (D, K) *UAS-eIF4E::HA*, (E, M) *UAS-lin-28::FLAG::HA*, (F, N) *UAS-pabp::FLAG*, (G) *UAS-rox8::FLAG::HA*, or (L) *UAS-FMR1::FLAG::HA* and stained for (A-G) FMRP or (H-N) ROX8. Note that overexpression of any of the above components fails to alter FMRP or ROX8 expression profiles, indicating that the above components are not sufficient for IPSG formation. (O-T) Gray scale confocal micrographs of 1mM sodium arsenite exposed progenitor cell pairs harboring esg-Gal4 and (O) *UAS-ago1::FLAG*, (P) *UAS-capr::FLAG::HA*, (Q) *UAS-dcr2*, (R) *UAS-eIF4E::HA*, (S) *UAS-pabp::FLAG*, (T) *UAS-rox8::FLAG::HA* and stained for (O-P, S-T) FLAG, (Q) DCR2 or (R) HA. (U-V) Fluorescent confocal micrographs of (U) control or (V) ATX2-overexpressing intestinal progenitor cells that are stained for (U-V and U'-V') OPP (red and gray), (U-V and U''-V'') HA (green and gray) and (U-V) DAPI. Note that ATX2 overexpressing cells have reduced OPP-staining indicating that nascent protein synthesis is downregulated.

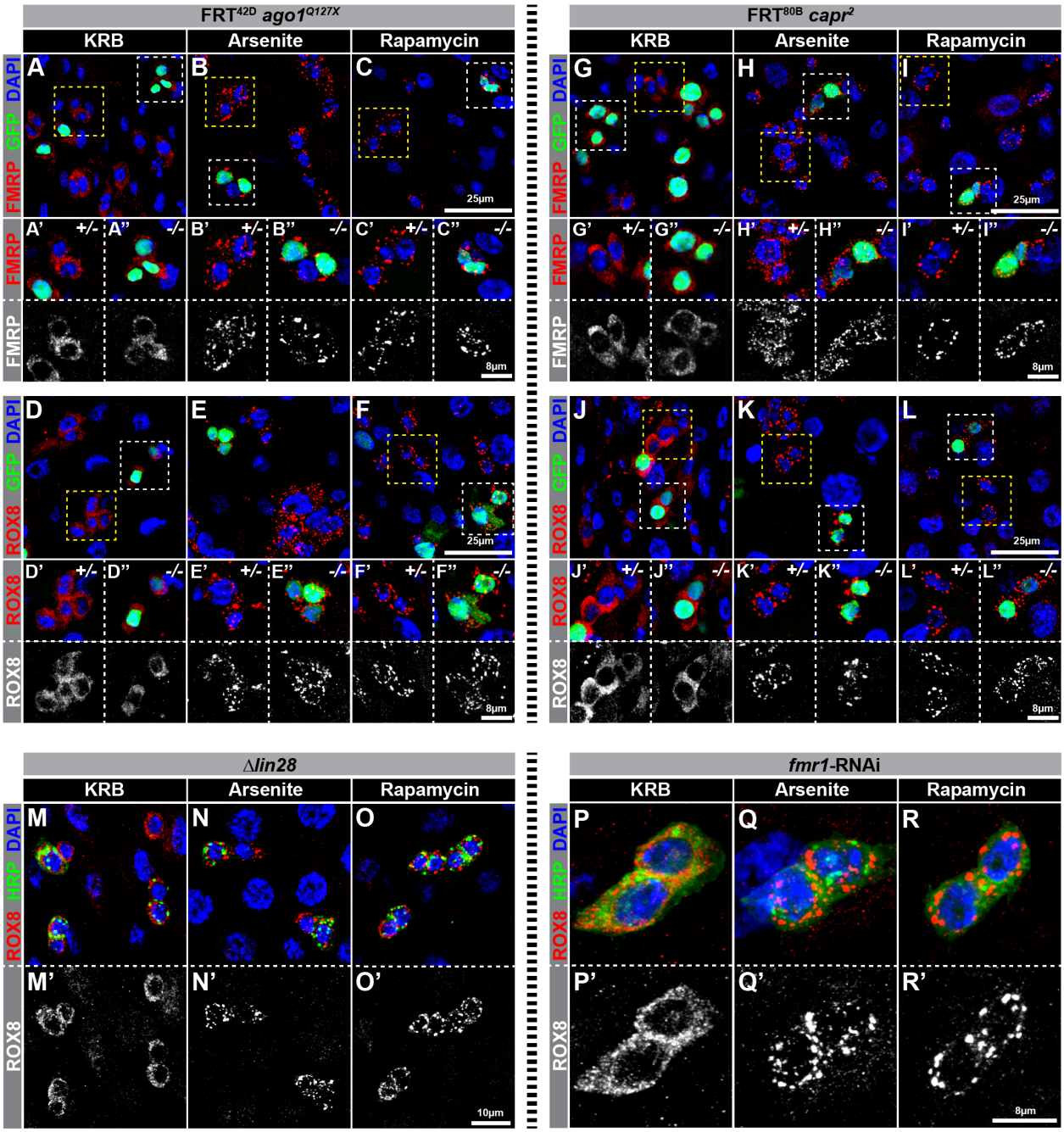

Figure S5: IPSGs form in intestinal progenitors deficient for *ago1, capr, lin-28 or fmr1*. (A-L) Confocal micrographs of intestinal cells homozygous (white boxes) or heterozygous (yellow boxes) for (A-F) *ago1*^{Q127X} or (G-L) *capr*^{2} null alleles and exposed to (A, D, G, J) KRB, (B, E, H, K) 1mM sodium arsenite, or (C, F, I, L) 1mM rapamycin and stained for (A-C, G-I) FMRP (red) or (D-F, J-L) ROX8 (red), (A-L) GFP (green) and (A-L) DAPI (blue). (A'-L') and (A''-L'') show insets of progenitor cells that are

heterozygous (GFP negative and outlined with the yellow box) or homozygous (GFP positive and outlined with the white box) for the *ago1*^{Q127X} (A-F) or *capr*^{2} (G-L) null allele. (M-O) Posterior midgut epithelia of *Δlin-28* intestines treated with (M) KRB, (N) 1mM sodium arsenite, or (O) 1mM rapamycin and stained for ROX8 (red in M-O, white in M'-O'), HRP (green), and DAPI (blue). (P-R) Pairs of intestinal progenitors from *esg-Gal4*, *UAS-fmr1-RNAi* intestines exposed to (P) KRB, (Q) 1mM sodium arsenite or (R) 1mM rapamycin and stained for ROX8 (red in P-R, white in P'-R'), HRP (green), and DAPI (blue). Note that IPSGs are formed in progenitors lacking either AGO1, CAPR, LIN-28 or FMRP.

Supplementary Tables

Table S1: Fly strains used in this study

Figure	Panels	Genotypes of flies used in each panel
Fig. 1	A, C-D, F-G, I-J	*gbe-smGFP::V5::nls / +*
	B	*gbe::LacZ / + ; atx2::GFP / +*
	E	*gbe-smGFP::V5::nls / + ; lin-28$^{\Delta 1}$, M{attP, lin-28^{RC}}ZH-86Fb / +*
	H	*gbe-smGFP::V5::nls / + ; HA::rin / +*
Fig. 2	A-D, F-G, I-J, L-M, O-P	*w^{1118}*
	E	*esg-Gal4 UAS-GFP tubGal80^{ts} / +*
	H	*atx2::GFP / +*
	K	*lin-28$^{\Delta 1}$, M{attP, lin-28^{RV}}ZH-86Fb / +*
	N	*HA::rin / +*
Fig. 3	A-F	*HA::rin*
Fig. 4	A-O	*HA::rin*
Fig. 5	A-E, K-M	*esg-Gal4 UAS-GFP tubGal80^{ts} / +*
	F-J, N-O	*HA::rin*
Fig. 6	A	*esg-Gal4 UAS-GFP tubGal80^{ts} / UAS-ago1::3xFLAG*
	B, K-Q	*esg-Gal4 UAS-GFP tubGal80^{ts} / + ; {UAS-atx2::3xHA}ZH-86Fb (F001031) / +*
	C	*esg-Gal4 UAS-GFP tubGal80^{ts} / UAS-capr::FLAG::HA*
	D	*esg-Gal4 UAS-GFP tubGal80^{ts} / UAS-dcr2*
	E	*esg-Gal4 UAS-GFP tubGal80^{ts} / +; {UAS-eIF4E::3xHA}ZH-86Fb (F000955) / +*
	F	*UAS-fmr1::FLAG::HA / + ; esg-Gal4 UAS-GFP tubGal80^{ts} / +*
	G	*UAS-lin28::FLAG::HA / + ; esg-Gal4 UAS-GFP tubGal80^{ts} / +*
	H	*esg-Gal4 UAS-GFP tubGal80^{ts} / + ; UAS-pabp::FLAG / +*
	I	*esg-Gal4 UAS-GFP tubGal80^{ts} / + ; UAS-rin::3xHA / +*
	J	*esg-Gal4 UAS-GFP tubGal80^{ts} / UAS-rox8::FLAG::HA*
Fig. 7	A-F	*hsFLP^{12} , tubGAL4, UAS-GFP / + ; P{lin-28 13kb::mCherry}attP40 / + ; FRT^{82B} tubP-GAL80^{LL3}/ FRT82B atx2^{x1}*
	G-L	*hsFLP^{12} , tubGAL4, UAS-GFP / + ; P{lin-28 13kb::mCherry}attP40 / + ; FRT^{82B} tubP-GAL80^{LL3}/ FRT82B rin^{3}*
	M-O	*Δrox8*
	P-T	*hsFLP^{12} , tubGAL4, UAS-GFP ; P{lin-28 13kb::mCherry}attP40 / + ; FRT^{82B} tubP-GAL80^{LL3} / FRT82B rin^{3}, atx2^{x1}, Δrox8*
Fig. S1	F, H, I	*w1118*
	G-I	*Δrox8*
	I	*hsFLP^{12} , tubGAL4, UAS-GFP / + ; P{lin-28 13kb::mCherry}attP40 / + ; FRT^{82B} tubP-GAL80^{LL3}/ FRT82B rin^{3}*
	I	*hsFLP^{12} , tubGAL4, UAS-GFP / + ; P{lin-28 13kb::mCherry}attP40 / + ; FRT^{82B} tubP-GAL80^{LL3}/ FRT82B atx2^{x1}*
	I	*hsFLP^{12} , tubGAL4, UAS-GFP / + ; P{lin-28 13kb::mCherry}attP40 / + ; FRT^{82B} tubP-GAL80^{LL3}/ FRT82B atx2^{x1}, Δrox8*
	I	*hsFLP^{12} , tubGAL4, UAS-GFP / + ; P{lin-28 13kb::mCherry}attP40 / + ; FRT^{82B} tubP-GAL80^{LL3}/ FRT82B rin^{3}, atx2^{x1}*
	I	*hsFLP^{12} , tubGAL4, UAS-GFP / + ; P{lin-28 13kb::mCherry}attP40 / + ;*

		FRT^{82B} tubP-GAL80^{LL3}/ FRT82B rin^{3}, Δrox8
	I	*hsFLP^{12} , tubGAL4, UAS-GFP / + ; P{lin-28 13kb::mCherry}attP40 / + ; FRT^{82B} tubP-GAL80^{LL3}/ FRT82B rin^{3}, atx2^{x1}, Δrox8*
Fig. S2	A-D	*piezo::Gal4, UAS-GFP, tubGal80^{ts} / + ; HA::rin / +*
Fig. S3	A-C	*w1118*
Fig. S4	A, H, O	*esg-Gal4 UAS-GFP tubGal80^{ts} / UAS-ago1::3xFLAG*
	B, I, P	*esg-Gal4 UAS-GFP tubGal80^{ts} / UAS-capr::FLAG::HA*
	C, J, Q	*esg-Gal4 UAS-GFP tubGal80^{ts} / UAS-dcr2*
	D, K, R	*esg-Gal4 UAS-GFP tubGal80^{ts} / +; {UAS-eIF4E::3xHA}ZH-86Fb (F000955) / +*
	L	*UAS-fmr1::FLAG::HA / + ; esg-Gal4 UAS-GFP tubGal80^{ts} / +*
	E, M	*UAS-lin28::FLAG::HA / + ; esg-Gal4 UAS-GFP tubGal80^{ts} / +*
	F, N, S	*esg-Gal4 UAS-GFP tubGal80^{ts} / + ; UAS-pabp::FLAG / +*
	G, T	*esg-Gal4 UAS-GFP tubGal80^{ts} / UAS-rox8::FLAG::HA*
	U-V	*esg-Gal4 UAS-GFP tubGal80^{ts} / + ; {UAS-atx2::3xHA}ZH-86Fb (F001031) / +*
Fig. S5	A-F	*hsFLP^{12} , tubGAL4, UAS-GFP / + ; FRT^{42D} tubP-GAL80^{LL2} / FRT42D ago1^{Q127X}*
	G-L	*hsFLP^{12} , tubGAL4, UAS-GFP / + ; ; FRT^{80B} tubP-GAL80^{LL3}/ FRT80B capr^{2}*
	M-O	*lin-28^{Δ1}*
	P-R	*esg-Gal4 UAS-GFP tubGal80^{ts} / + ; UAS-fmr1-RNAi (P{KK107935}VIE-260B) / +*

Table S2: Oligos used in this study

No.	Sequence	Additional Information
3144	GTTCGAAATCGATAAGCTTGGATC	Reverse oligo to dsRed
3202	AGCTCTTGGAAACCGGTTATGCGAGTGCACTTGGAAACCGGTTATGCGAGTTAACTTGGAAACCGGTTATGCGAGAGCTAAACTTACTTTCAGCTCGGTTCCCACGCCACTGCAAAACTTACTTTCAGCTCGGTTCCCACGCCACAAGCTTGCATGACGT	Top oligo that encodes 3XGBE and 2XSu(h) binding sites
3203	CATGCAAGCTTGTGGCGTGGGAACCGAGCTGAAAGTAAGTTTTGCAGTGGCGTGGGAACCGAGCTGAAAGTAAGTTTAGCTCTCGCATAACCGGTTTCCAAGTTAACTCGCATAACCGGTTTCCAAGTGCACTCGCATAACCGGTTTCCAAG	Bottom oligo that encodes 3XGBE and 2XSu(h) binding sites
3402	AAGAGCAGGCACAGAAGGCATCGCC	Amplifies *tra* nls from genomic DNA paired with 3421
3412	GCGCTGGCGATGCCTTCTGTGCCTGCTCTTGGTACTATCCAGTCCCAGCAACGGGTTCGG	Amplifies smGFP::V5 from pJFRC206 paired with 3416
3416	TCCTTTACTTCAGGCGGCCGCGGCTCGAGCAAAACATGGGAAAACCTATACCGAACCCCC	Amplifies smGFP::V5 from pJFRC206 paired with 3412
3421	AGTAAGGTTCCTTCACAAAGATCCTCTAGATACTTGTACAAGTTAGCGTCTTCGTTC	Amplifies *tra* nls from genomic DNA paired with 3402
3887	GAATACAAGAAGAGAACTCTGAATAACATGTATCCAGTTGGACAACAGTCACAG	Forward oligo to amplify *ago1* from SD07515 into pattB plasmid
3888	TAGTCGCCGTCGTGATCCTTGTAATCCGAACCGGCAAAGTACATGACCTTCTTGGTATCC	Reverse oligo to amplify *ago1* from SD07515 into pattB plasmid
4151	CTTCGCTTCGGTTGCGACTCGTCCA	Top oligo of gRNA 1 for *rox8* locus
4152	AAACTGGACGAGTCGCAACCGAAGC	Bottom oligo of gRNA 1 for *rox8* locus
4153	CTTCGCGGCGAAGGCTGCTGCGATT	Top oligo of gRNA for *rin* locus
4154	AAACAATCGCAGCAGCCTTCGCCGC	Bottom oligo of gRNA for *rin* locus
4158	AGCGGAGACAAAGAATCCGAGTCGAAGAGTCCGTAGTTCAGAGAGGAAGAATCAAACGCCAGCTATGTACCCATACGATGTGCCCGATTACGCCTACCCGTATGACGTCCCGGACTATGCCGTCATGGATGCGACGCAATCGCAGCAGCCTTCGCCGCAATCTGTGGGACGCGAGTTTGTCCGCCAGTACTACACGCTGT	ssODN repair template for *rin* locus containing 2XHA epitope tag
4179	AAGCGATGCAAGTGGTTGGGCGCC	Amplifies rin::ha fragment paired with 4184
4184	GATGTGCCCGATTACGCCTACCCG	Amplifies rin::ha fragment paired with 4179
4189	GAATACAAGAAGAGAACTCTGAATCAAAACAATGGACGAGTCGCAACCGAAGACCCTATA	Forward oligo to amplify *rox8* from FM011201 into pattB plasmid
4190	GTAGTCGCCGTCGTGATCCTTGTAATCTGCTTGGGTCTGGTATTGTGGCATCGCAGCACT	Reverse oligo to amplify *rox8* from FM011201 into pattB plasmid
4266	CCCTCTGTTGGGCCTGGACTCCACGGCGGCCGCACCTTCGGCTGCAAATACCGCTACTGT	Forward oligo to amplify *caprin* from LP14942 into pattB plasmid
4267	ACAGAAGTAAGGTTCCTTCACAAAGATCCTTCAGTTTTTGTTCTCCAGCCCGAGTGGCAT	Reverse oligo to amplify *caprin* from LP14942 into pattB plasmid

4285	ACGACCGAAAACCTGTATTTTCAGGGCGCCGACGAGTCGCAACCGAAG ACCCTATACGTG	Forward oligo to amplify *rox8* from FM011201 into pHIS.parallel
4286	ACTAGTTGAGCTCGTCGACGTAGGCCTTTGTCATTGGGTCTGGTATTGT GGCATCGCAGC	Reverse oligo to amplify *rox8* from FM011201 into pHIS.parallel
4309	CTTCGAAGACCCGCACGTCCTGGA	Top oligo of gRNA 2 for *rox8* locus
4310	AAACTCCAGGACGTGCGGGTCTTC	Bottom oligo of gRNA 2 for *rox8* locus
4384	AGCTACCCGCCCATCGCCCGGAGC	Reverse oligo to right of right homology arm sequence of *rox8*
4397	TGGGGTGTCGCCCTTCGCTGAAGCAGGTGGGCCCTCGTCTCGCTGGCG TGCCTGAGTGTG	Amplifies left homology from *rox8* locus paired with 4398
4398	CATGGCTGTCGGATGTCACGGGACTGTGGC	Amplifies left homology from *rox8* locus paired with 4397
4399	TAGTAAAGATCTCCATGCATAAGGCGCGCGCGGGTCTTCAAGGACAAG GGCTTCTCGTTC	Amplifies right homology from *rox8* locus paired with 4400
4400	ACTCGATTGACGGAAGAGCCTCGAGCTGCACAGTTGTCGCCGGCGTGG ATCACTTGAAGT	Amplifies right homology from *rox8* locus paired with 4399
4417	ACCGTGTGTGTCACCCGCCCGCCGG	Forward oligo to left of left homology arm sequence of *rox8*
4420	GATCTCCATGCATAAGGCGCGCGCG	Forward oligo to dsRed